Mobility Deficit Identification and Compensation through an Artificial Neural Network and Adaptive Controller Design during Gait

Silvia L. Chaparro-Cárdenas, Eduardo Castillo-Castañeda, and Alejandro A. Lozano-Guzmán

***Abstract*—This article presents a progressive compensation strategy for gait recovery in patients with different degrees of limited knee mobility, based on angular analysis and muscle electrical activity, and artificial intelligence. Ten subjects were tested during gait on a flat surface simulating 4 conditions of limited knee mobility with an active knee brace. Data on the amplitude of the electrical signal from 3 leg muscles were analyzed: rectus femoris, tibialis anterior, and gastrocnemius. In addition to the electromyography sensors, an angular position sensor was placed on the knee joint. An artificial neural network was trained to identify the type of limitation of each patient in their muscle activity. A knee orthosis with a linear actuator was designed to compensate for the loss of force during knee flexion-extension movement, according with limiting condition. The actuator trajectory is controlled through a model reference adaptive controller with a fuzzy logic-based adaptation mechanism. The simulation demonstrates the efficiency of this strategy, despite the high-amplitude disturbances in the system.**

Link to graphical and video abstracts, and to code: https://latamt.ieeer9.org/index.php/transactions/article/view/8957

***Index Terms*—Adaptive controller, Artificial neural network, Knee orthosis, Mobility deficit compensation.**

I. Introduction

In addition to accidents, some common diseases affect/weaken human gait. To help patients regain lower-limb mobility, physical therapists must analyse the cause of the limitation [1] and define a recovery protocol, including therapist-assisted repetitive exercises in early therapy [2]. Some mechatronic and robotic devices have been developed to assist patients in the phases of the gait cycle [3]. These devices use control strategies, human-computer interaction [4], dynamic analysis methods [5] according to the specific type of limitation both commercially and in research [6]–[8], are available. One of the most common control strategies for these devices is position control [9], where trajectories are defined by the therapist that establish the mobility capacity of the patient [10], after, each time the patient goes to therapy, the same procedure is redone, but with some variations depending on his progress [11]. To support the work of therapists, artificial intelligence and advanced control tools can be incorporated to detect the severity of the injury and control the amount of force to be applied during rehabilitation exercises. Currently, the automatic learning phase has been implemented to the feedback system, where safe trajectories are created [12]. Lokomat is one of the most used exoskeletons [13] for gait training and balance recovery therapies using an impedance control system to generate the appropriate trajectory for each patient [14].

Most gait assistance devices have been tested in healthy patients since their positive effects in a clinical setting is complicated [15]. However, the findings have been highly useful because these devices allow patients to experience different mobility patterns, thus helping their nervous system to learn trajectories [16]. A key requirement is that the control strategies implemented in rehabilitation devices match the therapeutic target, understanding each recovery task. In patients with mobility problems, diagnosis is highly complex. As such, an important control strategy is the use of Electromyographic (EMG) signals to interpret human muscle activation [17]. In [18], Akdogan et al. designed a knee rehabilitation device with a servo motor and with sensors integrating impedance control. The study by [19] comprehensively reviews control techniques used in lower-limb rehabilitation.

The main goal of our study is to compensate for muscle dysfunction during a gait protocol using a control algorithm by comparative analysis between healthy and impaired muscle function. For this purpose, a model of lower-limb flexion-extension motion is presented using muscular electrical activity assessed by leg EMG, kinematics and dynamics. This model correlates muscle electrical activity, characterised based on the Discrete Wavelet Transform (DWT) and on the lower-limb angle, with different levels of impairment using an Artificial Neural Network. Last, a Model Reference Adaptive Control (MRAC) algorithm for human gait dysfunction compensation is implemented through a knee orthosis with a degree of freedom that assists the flexion-extension motion. A fusion of Model Reference Adaptive Control – Proportional Integral Derivative – Fuzzy Control (MRAC-PID-Fuzzy) algorithms is obtained that use the kinematics and dynamics of the leg, the motor model, and the patterns that are extracted from the electromyography signals using Artificial Neural Network (ANN), progressive and safe movements are generated in

The associate editor coordinating the review of this manuscript and approving it for publication was Márcio J. Lacerda (*Corresponding author: Silvia Liliana Chaparro Cárdenas*).

This work was supported in part by the Consejo Nacional de Ciencia y Tecnología, México.

S. L. Chaparro-Cárdenas is with the Universidad de Investigación y Desarrollo UDI, San Gil, Colombia (e-mail: schaparro2@udi.edu.co).

E. Castillo-Castañeda, and A. A. Lozano-Guzmán are with the Instituto Politécnico Nacional, Querétaro 76090, México (e-mails: ecastilloca@ipn.mx, alozano@ipn.mx).

people with reduced mobility.

II. Related Works and Motivation

Control techniques applied to rehabilitation robotic devices, reported in the literature [20], have generated great reliable and safe results for people, especially considering the force control strategy and control techniques such as PID and MRAC. Currently, artificial intelligence techniques have been implemented in both lower and upper limb robotic devices for the process of data analysis and outcome prediction [21].

Major limitations have been identified in the development processes that do not allow the generation of individual trajectories for each person and their type of limitation. The trajectories used in the control systems are generated by a physiotherapist, who, at his discretion, considers and records the one that best suits the needs of each person. Broadly speaking, it is possible to identify that the autonomy of the devices has become one of the great challenges in the area. Their autonomy is limited to the energy capacity of the batteries and the feedback system that the device has [22]. This makes the gait trajectory unnatural, and it becomes repetitive movements for the patient, where he, in most cases, does not even interact.

EMG signals are a fundamental part of current control systems for the generation of active movements by the patient. Their muscle activity is obtained through electrodes when contracting and this information is used within a direct movement control process [23]. However, it is a topic that has not been thoroughly investigated because of the challenges involved. EMG signals are very noisy, variable and susceptible to external transfers, where, if the necessary techniques are not applied, they can be misinterpreted, completely affecting the accuracy of the overall device control system [24][25].

The portability of the device or exoskeleton is still a matter of discussion, since its weight, when instrumented, rises and generates load for the person. The objective is to find a comfortable design that can be used in an unlimited and safe way by any person.

III. Signal Acquisition During Gait

A. EMG Signal Acquisition

In this study, lower-limb muscles, thighs and legs, which are involved in a gait cycle [26], were selected using Surface Electromyography for the Non-invasive Assessment of Muscles (SENIAM) as a guide [27]. The rectus femoris (RF) muscle assists in hip flexion, leg flexion over the thigh, and knee extension [28]. The tibialis anterior (TA) muscle stabilises the ankle when touching the ground during the stance phase. Last, gait propulsion lies in the lateral gastrocnemius (LG) muscle, the main motor, which also causes plantar flexion of the foot and weakly contributes to leg flexion [29].

In addition to an angular-position sensor (potentiometer) in the knee joint (KJ), EMG electrodes were placed, in differential mode, considering the motor point of each muscle, as shown in Fig. 1 (a). The ankle is chosen as the reference point. The system uses MyoWare muscle sensors to record muscle electrical activity. The structure is attached to the body, allowing natural and comfortable mobility and avoiding biases in data collection as a result of the external agent used for data acquisition (see Fig. 1 (b)). The device has built-in amplifier and rectifier. The 2.5-cm-wide electrodes are disposable (AXELGAARD GEL), requiring no additional conductive gel, and universal transcutaneous electrical nerve stimulation (TENS)/EMG cables were used to acquire the signal. Using four sensors (1 potentiometer and 3 MyoWare muscle sensors), the gait cycle is measured starting with the right leg and recording four steps. To save the information, the system has a LiPo battery and a 3.3V voltage regulator, which feed a STM32 microcontroller that acquires data from the sensors and transmits this information via Bluetooth to the computer to generate the database. The signals were normalised from 0 to 1 as a function of the Maximum Voluntary Contraction (MVC) of each muscle, contracting for 5 seconds and raising the limb, and taking 60-second breaks, as shown in The ABC of EMG [29].

Fig. 2 shows EMG signals acquired for a four-step gait cycle for each selected muscle and for the potentiometer, which indicates the knee joint angle. The red curve corresponds to the signal acquired when the mobility is limited.

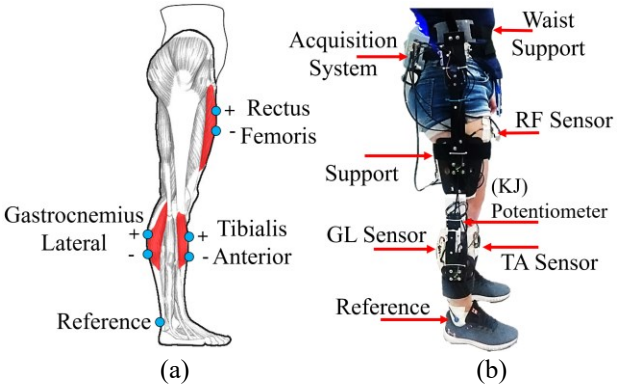

Fig. 1. Device and electronic instrumentation used: (a) location of the electrodes, (b) structure and location of the instrumentation.

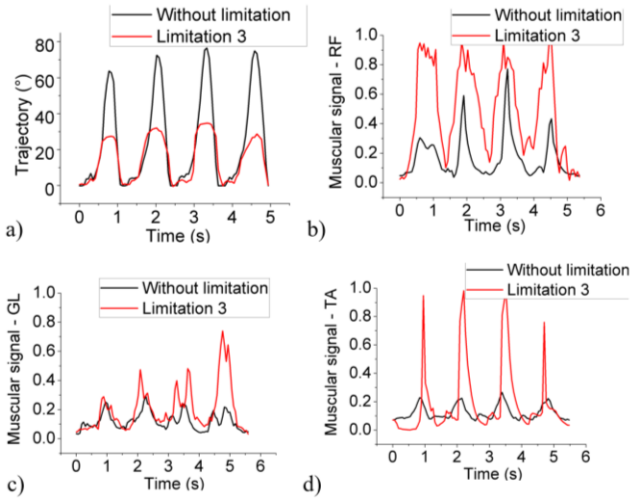

Fig. 2. EMG signals obtaining during a knee flexion-extension movement: (a) KJ reference trajectory, (b) RF, (c) GL, and (d) TA muscle.

B. Active Knee Support for Simulating Limited Mobility

A hinge-like active knee support (AKS) [30], attached to the

knee (see Fig. 3), generates a variable resistance force to through three independent torsion springs to simulate three levels of limited gait:

- Limitation 1: One spring, in the centre.
- Limitation 2: Two springs, at the ends.
- Limitation 3: Three springs.

The torsion constant for each limitation was calculated experimentally, finding values of 0.17, 0.28 and 0.36 [kg·m/rad], for limitations 1, 2 and 3, respectively.

Fig. 3. Hinge-like active knee support with torsion springs.

C. Data Acquisition in the Test Group

The test group consisted of 10 women aged between 22 and 28 years, with a mean ± standard deviation of 55 ± 5 kg weight and 155 ± 5 cm height. The participants reported that they were healthy people and that they had not had injuries or surgeries in the previous six months, in accordance with the Declaration of Helsinki [31] and local regulations. The inclusion criteria were being a woman and over 18 years of age; the exclusion criteria were using walking aids, such as crutches and canes, among others, being pregnant, and having had surgery in the lower limbs, been diagnosed with gait pathologies and altered gait for other diseases. Muscle electrical data was recorded from the right (dominant) leg of the participants. Data acquisition started when the participant began to walk with the right leg and ended when completing four steps. The test was performed on a flat surface and at a walking speed of approximately 3.6 km/h. The participants had to be able to withstand 2 kg, which is the combined weight of the data acquisition system and the AKS. This speed is lower than the normal gait speed due to the extra weight. To collect both angular and EMG data using the device that simulates the limitation, each subject completes the procedure with each AKS configuration, with 1-hour breaks for recovery between sets. After each test, the electrodes are removed, performing the cleaning protocol on each participant and on the structure. With data from the test group, for a gait trajectory (four steps), the effect of the three levels of limitation was quantified by measuring the maximum knee joint angle that each limitation allows (ψ_i) and the maximum angle at which pain is perceived (ϕ_i). In addition, the corresponding percentages were calculated, setting the angle ψ_N=107.2 (without limitation) to 100%. Last, the maximum increase μ_i which would avoid pain was calculated. The means are summarized in Table I. The value of μ_i was rounded to simplify its application in the controller.

The more severe the limitation is, the smaller the increase that can be applied in the progressive recovery trajectory of normal gait will be. Fig. 4 (a) shows the normal trajectory of the knee joint, which was used as a reference to generate the trajectories with limitation. Fig. 4 (b, c and d) show the trajectories for each limitation and knee joint (KJ) angle, expressed as ψ_i percentage (red lines), and the maximum trajectories before perceiving pain, expressed as μ_i percentage (blue lines) that will be used during the progressive recovery stage, which will allow the patient to exert herself to the maximum without pain.

TABLE I
ANGULAR DISPLACEMENT OF KNEE JOINT

	ψ_i [%]	ϕ_i [%]	$\mu_i = \phi_i - \psi_i$ [%]
No limitation (ψ_N)	100	-	-
Limitation 1	65.9	81.3	~ 16
Limitation 2	57.3	69.6	~ 12
Limitation 3	52.2	60.7	~ 7

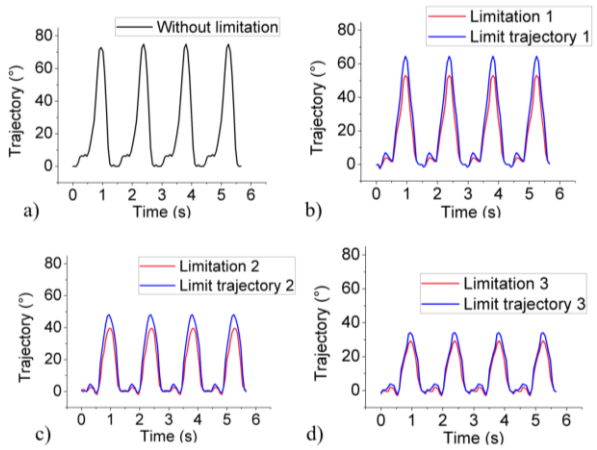

Fig. 4. Trajectory ranges per constraint to generate the maximum allowable progression: (a) Normal, (b) limitation 1, (c) limitation 2, (d) limitation 3.

III. EXPERIMENTAL SETUP

A. Neuronal Network Training

An ANN is a graph that mimics a brain in a simplified way. A neuron has several inputs, but only one output, representing a primitive model of biological neurons [32]. The ANN have been used successfully in classification problems with strongly nonlinear data. In mathematical terms, a neuron can be described by:

$$y = \varphi\left(\sum_{j=1}^{n} w_j x_j + b\right) \quad (1)$$

where x_j are the n input signals; w_j are the n synaptic weights of the neuron, b is the bias, φ is the activation function and y is the output signal. To determine the synaptic weights w_j, the ANN is trained with a set of known input and output values.

For ANN training the most widely used algorithm is backpropagation, which, valid iteratively changes the weights values using the magnitude of the partial derivative of the error:

$$\Delta w_{ij}(t) = \alpha X_i(t)\delta_i(t) \quad (2)$$

where α represents the learning rate, $X_i(t)$ are the inputs that propagate back to the i-th neuron at time t, and δ_i is the corresponding error gradient.

Effective training with ANNs is traditionally known for large amounts of data, but by making use of strategies, when the amount of data is limited, it is feasible to occupy them without overfitting the data. In this research, a simple ANN is configured as presented in Fig 5, with as few neurons as possible, thus avoiding overfitting.

The DWT is used to extract the information patterns of each of the EMG signals of people, both in the time and frequency domains, doing a real time analysis.

An ANN is used to identify the level of gait limitation of each test subject. The inputs are data extracted from the KJ potentiometer signals and from the EMG signals of the three muscle, a DWT is applied to each signal for compression. Therefore, a number of 8 DWT coefficients will be the input values of the ANN. For training, the ANN outputs will be the binary codes for the four types of gaits, as outlined in Table II. Considering that, for each subject in the test group, 4 signals were taken, corresponding to the RA, TA and LG muscles and the knee joint (KJ) angle and that the subjects can be classified into 4 classes, a vector is constructed whereby each subject labelled with a class has 32 characteristics, which is the product of the 8 coefficients of the 4 signal sources. For example, Table II outlines the 32 characteristics assessed in a test subject, through the DWT applied to one of the 4 signals. The 4 classes in Table III were simulated for each test subject, thereby totalling 40 data sets (as in Table II) for ANN training. The signals, now compressed using DWT, were classified by ANN configuration using the R Neuralnet package [33]. The resulting ANN model is shown in Fig. 5.

TABLE II
BINARY CODES BY LIMITATION TYPE

Class	Codification	Binary code
Normal	1	1 0 0 0
Limitation 1	2	0 1 0 0
Limitation 2	3	0 0 1 0
Limitation 3	4	0 0 0 1

TABLE III
COEFFICIENTS ESTIMATED USING DWT FOR ONE TEST SUBJECT

	KJ	RF	TA	GL
C1	14.128	0.087	0.145	0.572
C2	26.280	0.174	0.103	0.420
C3	49.002	0.305	0.279	0.494
C4	52.335	0.337	0.333	0.272
C5	58.230	0.252	0.226	0.699
C6	80.123	0.212	0.428	0.248
C7	25.599	0.069	0.290	0.403
C8	94.399	1.590	0.884	1.958

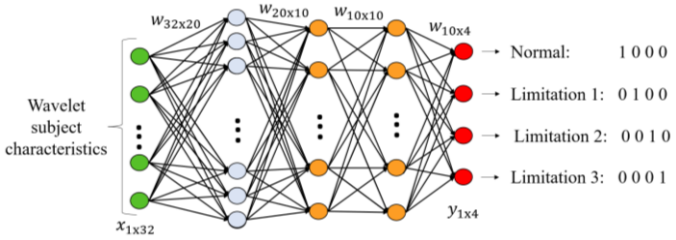

Fig. 5. ANN layers and input/output neurons.

The graph has 32 input neurons representing 8 DWT coefficients for each signal multiplied by 4 signals from the 3 MyoWare sensors and from the angular-position sensor. In total, 3 hidden layers are configured, the first layer with 20 nodes and the second and third layers with 10 nodes each. Last, 4 output neurons represent the 4 classes of the classifier (Normal, limitation 1, limitation 2 or limitation 3). Thus, a 40x32 data matrix was used to train and validate the ANN model, representing 40 objects, each of which with 32 characteristics and 4 values for class encoding.

Using R software's Caret package [34], the data set is partitioned into a training set (75%) and a test set (25%). In general, different runs were carried out varying some parameters, arbitrarily in order to obtain the best fit of the network and optimize the results based on the training data. The accuracy of the system is defined by the test percentage. The logistic activation function is selected considering the search for an approximation to a value and not a classification. Table IV presents the final configuration for the validation of all the data obtained in the experimentation stage.

The parameters were tuned through successive approximations observing the error obtained. The task of classifying or identifying the limitation level was performed at 90% accuracy. From this model, evaluation metrics using cross-validation with 13 subsets were derived from the confusion matrix, as shown in Table V. The Caret and ROCR packages of R are used for this purpose.

For this purpose, the Caret and ROCR packages of R were used [35]. The value of 0.6609623 is taken as threshold so that any value above that probability is taken as 1, and any value below as 0. The threshold is determined based on the ROCR package, which provides the optimal value for the model.

TABLE IV
ANN CONFIGURATION FOR NEURALNET

Parameter	Configuration
Iterations	1000
Learning rate	0.5 to 1.2
Algorithm	Backpropagation
Activation function	Logistic
Error equation	Quadratic error
Hidden layers	3 (20, 10, 10)

TABLE V
EVALUATION METRICS USING CROSS-VALIDATION WITH 13 SUBSETS

	Class 1	Class 2	Class 3	Class 4
Sensitivity	1.00	0.5	1.00	1.00
Specificity	0.88	1.00	1.00	1.00
Pos pred value	0.50	1.00	1.00	1.00
Neg pred value	1.00	0.85	1.00	1.00
Prevalence	0.10	0.40	0.30	0.20
Detection rate	0.10	0.30	0.30	0.20
Detection prevalence	0.20	0.30	0.30	0.20
Balanced accuracy	0.94	0.87	1.00	1.00

B. Knee Orthosis Description

To compensate for the movements that the patient cannot perform, due to the limitation level, an active knee orthosis was designed with a linear actuator containing an encoder as angular-position sensor, as shown in Fig. 6. The orthosis is firmly attached to the leg using an adjustable knee brace. The force generated by a DC motor enables the subject to compensate for the missing force and to follow the necessary path, gradually, depending on the type of limitation.

The orthosis was designed based on the AKS that was used to simulate mobility limitation, albeit without torsion springs. The linear actuator allows the knee to extend and flex in a controlled way to perform the gait cycle according to the type of limitation, previously identified by the ANN.

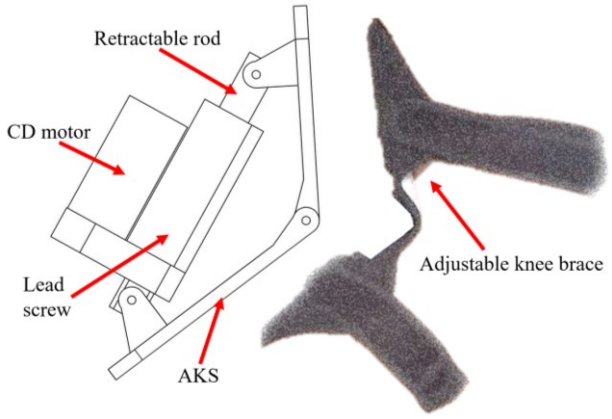

Fig. 6. Elements of the designed knee orthosis.

C. Adaptive Controller Design

To keep performance, when parameters change unpredictably over time, the controller must be adaptive [36][37]. MRAC works by adjusting the controller parameters so output of a reference model. The MRAC diagram implemented in this study consists of 5 blocks, as shown in Fig. 7. The Trajectory Generator and Adaptation Mechanism blocks use the type of limitation identified by the ANN as a parameter.

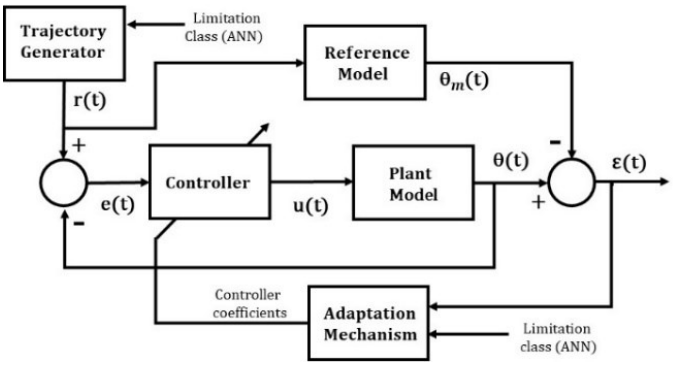

Fig. 7. MRAC block diagram.

- *Trajectory Generator*

The knee joint angle should follow a normal trajectory $y_N(t)$; however, depending on the type of limitation, the patient will perform only a percentage of $y_N(t)$, that is:

$$r(t) = \psi_i y_N(t) \tag{3}$$

Where ψ_i is the percentage of limitation i (see Table 1). Always, the percentage of increase in trajectory must not exceed μ_i to prevent the patient pain.

- *Plant Model*

In a knee rehabilitation process, the patient generates most of the force necessary to perform the gait cycle. Depending on the level of limitation, the orthosis (through a DC motor) must provide the complementary force. Therefore, the plant will consist of a DC motor, where the input is the supply voltage $U(s)$ and the output will be the orthosis angle $\theta(s)$. Eq. 4 shows the transfer function of the plant, which relates these two variables and the parameters of the DC motor. In the Eq. 4, the authors consider $T_E(s) = 0$, where $T_E(s)$ is the external torque generated by the patient's leg.

$$\frac{\theta(s)}{U(s)} = \frac{K_m}{[L_a J_m s^2 + (L_a B_m + R_a J_m)]s^2 + (R_a B_m + K_b K_m)} \tag{4}$$

The constants values, $K_m, L_a, R_a, J_m, B_m, K_b$, are derived from the datasheet of the motor that operates the orthosis (see Table VI).

Fig. 8 shows the MRAC torque diagram, considering a closed-loop control system. The final torque obtained to generate the motion is the sum of torques of the motor $T_M(s)$ and the person's leg $T_E(s)$.

The blocks are composed of first order equations, the electromotive force constant (EMF), the leg torque and to obtain an output in the required units (position), the velocity integral block is added at the end.

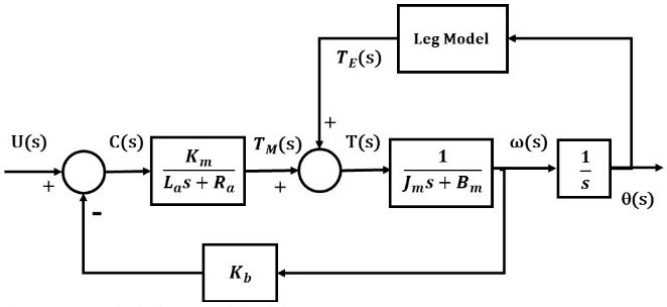

Fig. 8. Extended plant model of the MRAC.

TABLE VI
DC MOTOR PARAMETERS

Parameter	Description	Value	Units
K_m	Torque constant	0.05	Nm/A
L_a	Inductance	0.046	H
R_a	Resistance	1	Ω
J_m	Inertia	0.093	Kgm^2
B_m	Friction constant	0.08	Nms/rad
K_b	EMF constant	0.05	Vs/rad

To approximately represent a patient's leg, a model was used in SolidWorks; the estimated inertia matrix is:

$$I_T = \frac{m_e L_e^2}{12}\begin{bmatrix}0 & 1 & 0\\ 0 & 1 & 1\\ 1 & 0 & 1\end{bmatrix} \quad (5)$$

where m_e is the average mass of the leg (3.25 kg), and L_e is the average length of the leg (0.57 m), for the subject group.

In this way, the torque generated by the leg, while the knee rotates an angle θ(t) is:

$$T_E(t) = \frac{L_e^2 m_e(2L_e^2 + L_e + 1) + 2L_e y_E(t)}{4} + \frac{2L_e^3 m_e + 1}{12} \quad (6)$$

$$y_E(t) = g m_e \cos(\theta(t)) \quad (7)$$

For example, Fig. 9 shows the curves of the simulated torque for the three types of limitation, considering the maximum percentage of increase allowed.

- *Controller*

The control used in this study consisted of a PID controller, which generates an output (control signal u(t)):

$$\frac{U(s)}{E(s)} = P + \frac{I}{s} + Ds \quad (8)$$

The values of the coefficients used in simulation, for each level of limitation, are presented in Table VII.

However, the lack of knowledge on the model of the patient's leg and the variability in the test group require a robust control to maintain the desired performance.

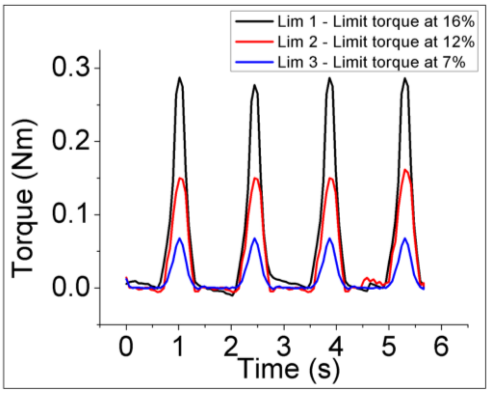

Fig. 9. Simulated external torque by type of limitation.

TABLE VII
CONTROL COEFFICIENTS BY TYPE OF LIMITATION

Limitation	P	I	D
1	3.44	18.8	10.2
2	3.44	18.8	10.2
3	0.7	40.5	20.8

The simulations demonstrated that P coefficient alone is sufficient to reject disturbances or inaccuracies in the model. Therefore, the adaptation mechanism concerns only P value.

- *Adaptation Mechanism*

The controller coefficients were adjusted using fuzzy logic to estimate P and to reduce the error $\varepsilon(t) = \theta(t) - \theta_m(t)$, (see Fig. 8) generated by the poor knowledge on the plant model. For both input and output, 5 fuzzy sets were used. To a fast response, trapezoidal membership functions were implemented at the ends and middle of the fuzzy and triangular sets in the centre, which was the best configuration for reducing the error. To improve the result, a couple of membership functions are proposed for each type of limitation (see Fig. 10, 11, and 12).

In fuzzy input sets, BN is big negative, SN is small negative, Ze is zero, SP is small positive, and BP is big positive. In the output sets of the same Figures, BD is big decrease, SD is small decrease, Z is zero, SI is small increase, and BI is big increase. The rule base, consisting of 5 if-then rules (see Table VIII).

The Mamdani inference system, the Maximum aggregation method and the centroid defuzzification method with sigmoid behaviour were used in this study.

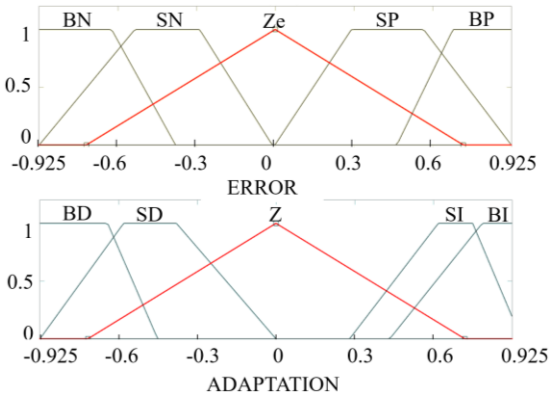

Fig. 10. Membership functions for limitation 1.

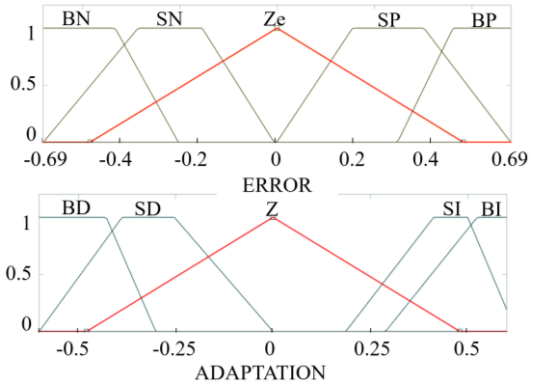

Fig. 11. Membership functions for limitation 2.

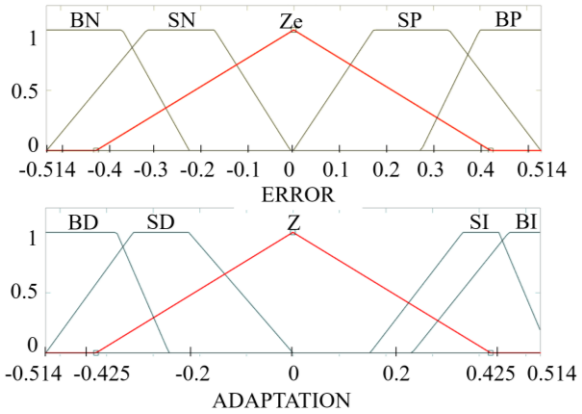

Fig. 12. Membership functions for limitation 3.

TABLE VIII
USED FUZZY RULE BASE FOR THE ADAPTATION MECHANISM

Number	Rule
1	If Error is BN then Adaptation is BD
2	If Error is SN then Adaptation is SD
3	If Error is Ze then Adaptation is Z
4	If Error is SP then Adaptation is SI
5	If Error is BP then Adaptation is BI

- *Reference Model*

The final objective of the control system is to consider in the output the original trajectory of the person coming from the two branches, as shown in Fig 7: [1]the one passing through the control blocks and [2]the trajectory of the reference model.

In the reference model, we have a transfer function Eq. 9, which aims to smooth the input trajectory of the system with controlled movements that ensure the articulation of the person. This transfer function is arranged under physiological reasons for its choice in the block system. To select the transfer function of this block, we chose an overshoot of 20% and a peak time of 0.04 seconds for the response to a unit step input. Thus, the transfer function for the reference model block is:

$$\frac{\theta_m(s)}{R(s)} = \frac{3337}{s^2+52s+3337} \tag{9}$$

IV. RESULTS

Five percentages μ_i of increase were selected for each limitation, emulating a progressive rehabilitation. The control performance was observed before a pulse-type disturbance with an amplitude of 0.15 radians and lasting 0.5 seconds.

Figure 13 shows the error for each limitation with (in black colour) and without (in red colour) adaptation mechanism, for a single percentage per limitation. Fig 13 (a). shows the graph of the knee trajectory without constraint. Fig 13 (b) presents the percentage error during constraint trajectory 1, in this the error is maximum 2.27° without perturbation and 3.12° with perturbation. Fig 13 (c) presents the percentage error during the trajectory of constraint 2, obtaining a maximum error of 1.44° without perturbation and 2.42° with perturbation. Fig 13 (d) shows the error obtained during the constraint 3 trajectory. In this trajectory, 0.93° is obtained without perturbation and 2.01° with perturbation. The higher the limitation, the lower the error percentage, and this is due to: 1 the degree of spasticity or stiffness of the limb, 2 the speed and amplitude with which the limb goes, the control system is able to react faster.

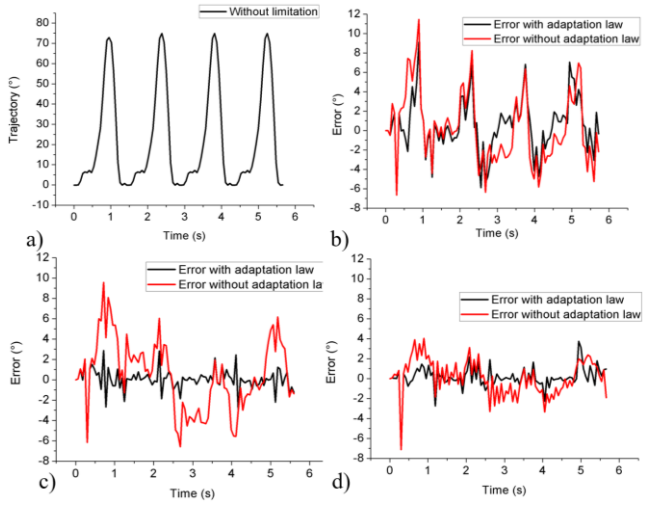

Fig. 13. Errors with and without adaptation: a) normal trajectory, b) limitation 1, c) limitation 2, d) limitation 3.

Table IX shows the error assessed for 5 percentages, for each limitation, with and without applying the disturbance. The largest percentage corresponds to the maximum value at which the patient perceives pain.

The MRAC-PID-Fuzzy control technique proved to be efficient because its mean square error was relatively low despite the high-amplitude disturbance in the system. The configuration presented, both of the ANN and the control system, can be used for data from other people, considering the characteristics mentioned above (section 2.4).

The MRAC-PID-Fuzzy control has a high capacity for adaptation and response to any modification or disturbance, which makes it highly scalable. As blocks were added, the efficiency of the system was tested, finding that a single control technique was not sufficient to obtain the results expected by the authors. When testing with PID control, it failed especially when the control gain increased.

TABLE IX
ERROR ASSESSED FOR 5 PERCENTAGES BY TYPE OF LIMITATION

Limitation type	%	Error (°)	
		Without disturbance	With disturbance
1	0	1.67	2.80
	4	2.27	2.86
	8	2.05	3.08
	12	1.05	3.11
	16	2.17	3.12
2	0	1.13	2.29
	3	1.34	2.29
	6	1.44	2.33
	9	0.95	2.42
	12	0.72	2.39
3	0	0.84	0.40
	2	0.69	0.94
	4	0.56	1.57
	6	0.52	2.01
	7	0.93	1.85

Narayan J. et al, in [5] propose a passive PID control, by the patient, with a neurofuzzy compensation phase, in which they simulate having a patient in their exoskeleton device. Its control system is based on the Euler-Lagrange method for generating exoskeleton movements, and the stability of the control system is mathematically demonstrated with the Lyapunov theorem. We are at a point where a combination of sensors is required that provide information not only about the robotic device but about the person, in order to objectively evaluate their physical progress [12].

V. CONCLUSION

Muscle electrical activity was analysed through an ANN model during a gait protocol in subjects with normal gait and with some level of limitation, considering the knee flexion-extension angle. By knowing the trajectories of each type of limitation and the percentages of movement that each subject can bear, progressive training routines can be proposed by gradually increasing the trajectories. Control techniques, such as that applied in this study, allow mechanical support devices to operate safely.

While EMG signals have characteristics that can visually differ from one subject to another, algorithms such as ANNs, within their mathematical approximations, can find patterns or similarities that are useful in control systems. With this ANN model, which has an average accuracy of 97.5%, sufficient reliability is provided to know whether the gait shows some limitation and to subsequently apply strategies for progressive recovery, through robust devices and controls.

The MRAC-PID-FUZZY control strategy shows satisfactory results because EMG and knee position signals make it is possible to identify gait limitations and to establish trajectories with a safe increase that can be used for normal gait recovery. The next stage of this study is to build an actuated knee orthosis to experimentally validate our proposal.

To obtain better results between the connections between layers of the neural network and validate the proposed artificial intelligence models, algorithms with associative memory have been created. These have demonstrated better results in the optimization process, precision and specificity using the logical mining model [38], which surpasses the theoretical and empirical references of any data set.

The number of people who participated in the experimentation may be considered small to generalize about a control technique. However, with these data it is possible to obtain a first approximation of a control technique that considers within its feedback system EMG signals from individuals and generates progressive trajectories according to the limitation. To obtain a more generalized model, it is recommended to expand the population and include a previous evaluation of the test subjects by a physiotherapist and assess whether they are healthy or present some type of limitation. Similarly, the results should be analysed by a physiotherapist to determine their reliability.

To evaluate the performance of the configuration proposed in this article, a set of unknown data is necessary, which can be considered in future research. However, artificial neural networks are robust models based on supervised learning methodologies, showing acceptable results against irrelevant predictors.

The results obtained in this paper with the selected ANN configuration are very good. However, other simpler techniques such as logistic regression or other ANN architectures can be applied and more simplified models for limitation identification can be obtained.

In future work, one may consider changing only the control technique and retesting with the same trajectories to compare the error with and without perturbation.

ACKNOWLEDGMENTS

The authors would like to thank to the Consejo Nacional de Ciencia y Tecnología, México, and Universidad de Investigación y Desarrollo - UDI; from their support in the realization of this work.

REFERENCES

[1] Y. H. Bae, W. H. Chang, and S. S. M. Fong, "Different effects of robot-assisted gait and independent over-ground gait on foot plantar pressure in incomplete spinal cord injury: A preliminary study," *Int. J. Environ. Res. Public Health*, vol. 18, no. 22, pp. 6–13, 2021, doi: 10.3390/ijerph182212072.

[2] H. Zhang *et al.*, "Three-Dimensional Gait Analysis and sEMG Measures for Robotic-Assisted Gait Training in Subacute Stroke: A Randomized Controlled Trial," *Biomed Res. Int.*, vol. 2023, pp. 1–12, 2023, doi: 10.1155/2023/7563802.

[3] A. M. Abdullahi and R. Chaichaowarat, "Sensorless Estimation of Human Joint Torque for Robust Tracking Control of Lower-Limb Exoskeleton Assistive Gait Rehabilitation," *J. Sens. Actuator Networks*, vol. 12, no. 4,

2023, doi: 10.3390/jsan12040053.

[4] W. Wang, T. Gong, Z. Song, Z. Wang, and J. Ji, "Simulation study on assist-as-needed control of a rehabilitation robotic walker," *Technol. Health Care*, vol. 31, no. S1, pp. 293–302, 2023, doi: 10.3233/THC-236025.

[5] J. Narayan and S. K. Dwivedy, "Towards Neuro-Fuzzy Compensated PID Control of Lower Extremity Exoskeleton System for Passive Gait Rehabilitation," *IETE J. Res.*, vol. 69, no. 2, pp. 778–795, 2023, doi: https://doi.org/10.1080/03772063.2020.1838346.

[6] J. Cao, S. Q. Xie, R. Das, and G. L. Zhu, "Control strategies for effective robot assisted gait rehabilitation: The state of art and future prospects," *Medical Engineering and Physics*, vol. 36, no. 12. Elsevier Ltd, pp. 1555–1566, Dec. 01, 2014, doi: 10.1016/j.medengphy.2014.08.005.

[7] M. S. H. Bhuiyan, I. A. Choudhury, and M. Dahari, "Development of a control system for artificially rehabilitated limbs: a review," *Biol. Cybern.*, vol. 109, no. 2, pp. 141–162, 2015, doi: 10.1007/s00422-014-0635-1.

[8] S. Hussain, P. K. Jamwal, and M. H. Ghayesh, "Single joint robotic orthoses for gait rehabilitation: an educational technical review," *J Rehabil Med*, vol. 48, no. 36, pp. 333–338, 2016, doi: 10.2340/16501977-2073.

[9] W. Meng, Q. Liu, Z. Zhou, Q. Ai, B. Sheng, and S. (Shane) Xie, "Recent development of mechanisms and control strategies for robot-assisted lower limb rehabilitation," *Mechatronics*, vol. 31, pp. 132–145, 2015, doi: 10.1016/j.mechatronics.2015.04.005.

[10] J. Cao, S. Quan, R. Das, and G. L. Zhu, "Control strategies for effective robot assisted gait rehabilitation : The state of art and future prospects," *Med. Eng. Phys.*, vol. 36, no. 12, pp. 1555–1566, 2014, doi: 10.1016/j.medengphy.2014.08.005.

[11] V. Dietz, T. Nef, and W. Z. Rymer, "Technology of the Robotic Gait Orthosis Lokomat," *Neurorehabilitation Technol.*, vol. 19, no. 1, pp. 395–407, 2016, doi: 10.1007/s13398-014-0173-7.2.

[12] D. Su, Z. Hu, J. Wu, P. Shang, and Z. Luo, "Review of adaptive control for stroke lower limb exoskeleton rehabilitation robot based on motion intention recognition," *Front. Neurorobot.*, vol. 17, pp. 1–21, 2023, doi: 10.3389/fnbot.2023.1186175.

[13] F. Artoni, A. Cometa, S. Dalise, V. Azzollini, S. Micera, and C. Chisari, "Cortico-muscular conncectivity is modelated by passive and active Lokomat-assisted Gait," *Nat. Portf.*, vol. 13, pp. 1–13, 2023, doi: https://doi.org/10.1038/s41598-023-48072.

[14] S. Jezernik, G. Colombo, T. Keller, H. Frueh, and M. Morari, "Robotic Orthosis Lokomat : A Rehabilitation and Research Tool," *Int. Neuromodulation Soc.*, vol. 6 no. 2, no. 3, pp. 108–115, 2003, doi: 1094-7159/03.

[15] J. L. Emken, S. J. Harkema, J. A. Beres-Jones, C. K. Ferreira, and D. J. Reinkensmeyer, "Feasibility of manual teach-and-replay and continuous impedance shaping for robotic locomotor training following spinal cord injury," *IEEE Trans. Biomed. Eng.*, vol. 55, no. 1, pp. 322–334, 2008, doi: 10.1109/TBME.2007.910683.

[16] S. K. Banala, A. Kulpe, and S. K. Agrawal, "A powered leg orthosis for gait rehabilitation of motor-impaired patients," *Proc. - IEEE Int. Conf. Robot. Autom.*, no. April, pp. 4140–4145, 2007, doi: 10.1109/ROBOT.2007.364115.

[17] G. Kwakkel, B. J. Kollen, and R. C. Wagenaar, "Therapy Impact on Functional Recovery in Stroke Rehabilitation: A critical review of the literature," *Physiotherapy*, vol. 85, no. 7, pp. 377–391, 1999, doi: 10.1016/S0031-9406(05)67198-2.

[18] E. Akdogan and M. A. Adli, "The design and control of a therapeutic exercise robot for lower limb rehabilitation: Physiotherabot," *Mechatronics*, vol. 21, no. 3, pp. 509–522, 2011, doi: 10.1016/j.mechatronics.2011.01.005.

[19] S. L. Chaparro-Cárdenas, A. A. Lozano-Guzmán, J. A. Ramirez-Bautista, and A. Hernández-Zavala, "A review in gait rehabilitation devices and applied control techniques," *Disabil. Rehabil. Assist. Technol.*, vol. 13, pp. 819–834, 2018, doi: 10.1080/17483107.2018.1447611.

[20] J. Narayan, C. Auepanwiriyakul, S. Jhunjhunwala, M. Abbas, and S. K. Dwivedy, "Review Hierarchical Classification of Subject-Cooperative Control strategies for Lower Limb Exoskeletons in Gait Rehabilitation: A Systematic Review," *machines*, vol. 11, no. 764, pp. 1–20, 2023, doi: 10.3390/machines11070764.

[21] E. J. Harris, I.-H. Khoo, and E. Dernircan, "A Survey of Human Gait-Based Artificial Intelligence Applications," *Front. Robot. AI*, vol. 8, pp. 1–28, 2022, doi: 10.3389/frobt.2021.749274.

[22] H. Zhang, Z. Chen, D. Zanotto, and Y. Guo, "Robot-Assisted and Wearable Sensor-Mediated Autonomous Gait Analysis," *IEEE International Conference on Robotics and Automation (ICRA)*. Paris, France, pp. 6795–6802, 2020, doi: 10.1109/ICRA40945.2020.9197571.

[23] C. Lu *et al.*, "Multi-Channel FES Gait Rehabilitation Assistance System Based on Adaptive sEMG Modulation," *IEEE Trans. Neural Syst. Rehabil. Eng.*, vol. 31, pp. 3652–3663, 2023, doi: 10.1109/TNSRE.2023.3313617.

[24] N. A. El Yaakoubi, C. McDonald, and O. Lennon, "Review Prediction of Gait Kinematics and Kinetics: A Systematic Review of EMG and EEG Signal Use and Their Contribution to Prediction Accuracy," *bioengineering*, vol. 10, pp. 1–23, 2023, doi: 10.3390/bioengineering10101162.

[25] N. Nazmi, S.-I. Yamamoto, M. A. S. Rohim, and E. F. Shair, "Classification of Gait Phases by Using SVM and ANN Based on EMG Signals," *IEEE Symposium on Industrial Electronics & Applications (ISIEA)*, Malaysia, pp. 1–6, 2024.

[26] M. B. I. Raez, M. S. Hussain, F. Mohd-Yasin, M. Reaz, M. S. Hussain, and F. Mohd-Yasin, "Techniques of EMG signal analysis: detection, processing, classification and applications.," *Biol. Proced. Online*, vol. 8, no. 1, pp. 11–35, 2006, doi: 10.1251/bpo115.

[27] H. J. Hermens *et al.*, *European Recommendations for Surface ElectroMyoGraphy*, vol. 8. Roessingh Research and Development b.v., 1999.

[28] M. S. Hussain, M. B. I. Reaz, and M. I. Ibrahimy, "Electromyography signal analysis using wavelet transform nd higher order statistics to determnine muscle contraction," *Expert Syst.*, vol. 26, no. 1, pp. 35–48, 2009, doi: 10.1111/j.1468-0394.2008.00483.x.

[29] P. Konrad, *The ABC of EMG A Practical Introduction to Kinesiological Electromyography*. Scottsdale, Arizona, 2006.

[30] NASUS SPORTS, "Powerknee brace," 2021. https://nasus-sports.com/products/powerknee-brace.

[31] Helsinki, "Declaration of Helsinki World Medical Association Declaration of Helsinki," *World Heal. Organ.*, vol. 79, no. October 1975, pp. 373–374, 2001.

[32] P. Fuangkhon, "An incremental learning preprocessor for feed-forward neural network," *Artif. Intell. Rev.*, vol. 41, no. 2, pp. 183–210, 2014, doi: 10.1007/s10462-011-9304-0.

[33] Stefan Fritsch, Frauke Guenther, Marvin N. Wright, Marc Suling, and Sebastian M. Mueller, "Package 'neuralnet' Training of Neural Networks," pp. 1–15, 2019, [Online].

Available: https://cran.r-project.org/web/packages/neuralnet/neuralnet.pdf.

[34] M. Kuhn *et al.*, "Package ' caret ' R topics documented :" pp. 1–223, 2020, [Online]. Available: https://github.com/topepo/caret/.

[35] T. Sing, O. Sander, N. Beerenwinkel, T. Lengauer, T. Unterthiner, and F. G. M. Ernst, "'Package ROCR' - Visualizing the Performance of Scoring Classifiers." pp. 1–15, 2020.

[36] P. Jain and N. M.J, "Design of a Model Reference Adaptive Controller Using Modified MIT Rule for a Second Order System," *Adv. Electron. Electr. Eng.*, vol. 3, no. 4, pp. 477–484, 2013, doi: 2231-1297.

[37] A. Shekhar and A. Sharma, "Review of Model Reference Adaptive Control," in *2018 International Conference on Information , Communication, Engineering and Technology (ICICET)*, Aug. 2018, pp. 1–5, doi: 10.1109/ICICET.2018.8533713.

[38] N. E. Zamri *et al.*, "A modified reverse-based analysis logic mining model with Weighted Random 2 Satisfiability logic in Discrete Hopfield Neural Network and multi-objective training of Modified Niched Genetic Algorithm," *Expert Syst. Appl.*, vol. 240, p. 122307, 2024, doi: https://doi.org/10.1016/j.eswa.2023.122307.

Silvia L. Chaparro-Cárdenas received the electronic engineer degree with the with a specialty in process control from the Fundación Universitaria de San Gil UNISANGIL, Colombia, in 2013. The master degree and the Ph.D. degree in advanced technology, with a speciality in mechatronics, from the Centro de Investigación en Ciencia Aplicada y Tecnología Avanzada (CICATA), Instituto Politécnico Nacional, Mexico, in 2016 and 2021, respectively. Her research interests include fuzzy systems, hybrid systems, robotic rehabilitation devices, neural networks, artificial intelligence, signal processing and intelligent control. She has published articles in in data analysis, control systems and artificial intelligence. She is currently full-time professor at the Universidad de Investigación y Desarrollo UDI, in Colombia.

Eduardo Castillo-Castañeda, a Mechanical Electrical Engineer, graduated from Universidad Nacional Autonoma de Mexico in 1987. In 1994 he received his Ph.D. in Automatic Control from the Institute National Polytechnique de Grenoble, France. In 2015, he received the Training Certificate "Leaders in Innovation" by the Royal Academy of Engineering and the University of Oxford, in the United Kingdom. Currently, he is member of the Technical Committee for Robotics and Mechatronics of IFToMM, the International Federation for the Promotion of Mechanism and Mechanics Science. Since 2007, he is full time professor at the Instituto Politécnico Nacional, in Mexico.

Alejandro A. Lozano-Guzmán received the B.S. in Mechanical and Electrical Engineering degree at the Mexico National University, 1975 and the M.S degree in Mechanical Engineering, at the same University in 1977. He obtained the Ph.D. in Mechanical Engineering, University of New Castle Upon Tyne, England in 1982. He is a Professor at CICATA Querétaro, in México. His research focusses on mechanical systems analysis, particularly mechanical vibrations and condition monitoring systems. He has published articles in mechanical systems analysis and is a member of the National Research System.